

In-situ ultrasonic calibrations of pressure and temperature in a hinge-type double-stage cubic large volume press

Qingze Li(李青泽), Xiping Chen(陈喜平), Lei Xie(谢雷), Tiexin Han(韩铁鑫), Jiacheng Sun(孙嘉程), and Leiming Fang(房雷鸣)

Citation: Chin. Phys. B, 2022, 31 (**6**): 060702. DOI: 10.1088/1674-1056/ac4902
Journal homepage: http://cpb.iphy.ac.cn; http://iopscience.iop.org/cpb

What follows is a list of articles you may be interested in

Investigating the thermal conductivity of materials by analyzing the temperature distribution in diamond anvils cell under high pressure

Caihong Jia(贾彩红), Min Cao(曹敏), Tingting Ji(冀婷婷), Dawei Jiang(蒋大伟), and Chunxiao Gao(高春晓)
Chin. Phys. B, 2022, 31 (**4**): 040701. DOI: 10.1088/1674-1056/ac29aa

A double-layer heating method to generate high temperature in a two-stage multi-anvil apparatus

Bo Peng(彭博), Zili Kou(寇自力), Mengxi Zhao(赵梦溪), Mingli Jiang(姜明莉), Jiawei Zhang(张佳威), Yipeng Wang(王义鹏), Lu Zhang(张陆)
Chin. Phys. B, 2020, 29 (**9**): 090703. DOI: 10.1088/1674-1056/ab9dec

The design of 2/8-type high-pressure cell applied to *in situ* neutron diffraction

Chun-Jiang Xiang(向春江), Qi-Wei Hu(胡启威), Qiang Wang(王强), Lei Xie(谢雷), Xi-Ping Chen(陈喜平), Lei-Ming Fang(房雷鸣), Duan-Wei He(贺端威)
Chin. Phys. B, 2019, 28 (**7**): 070701. DOI: 10.1088/1674-1056/28/7/070701

Pressure-induced phase transition of B-type Y_2O_3

Qian Zhang(张倩), Xiang Wu(巫翔), Shan Qin(秦善)
Chin. Phys. B, 2017, 26 (**9**): 090703. DOI: 10.1088/1674-1056/26/9/090703

A-site ordered perovskite$CaCu_3Cu_2Ir_2O_{12-\delta}$ with square-planar and octahedral coordinated Cu ions

Qing Zhao(赵庆), Yun-Yu Yin(殷云宇), Jian-Hong Dai(戴建洪), Xi Shen(沈希), Zhi-Wei Hu(胡志伟), Jun-Ye Yang(杨俊叶), Qing-Tao Wang(王清涛), Ri-Cheng Yu(禹日成), Xiao-Dong Li(李晓东), You-Wen Long(龙有文)
Chin. Phys. B, 2016, 25 (**2**): 020701. DOI: 10.1088/1674-1056/25/2/020701

In-situ ultrasonic calibrations of pressure and temperature in a hinge-type double-stage cubic large volume press

Qingze Li(李青泽), Xiping Chen(陈喜平), Lei Xie(谢雷),
Tiexin Han(韩铁鑫), Jiacheng Sun(孙嘉程), and Leiming Fang(房雷鸣)[†]

Key Laboratory for Neutron Physics, Institute of Nuclear Physics and Chemistry, China Academy of Engineering Physics, Mianyang 621900, *China*

(Received 2 November 2021; revised manuscript received 27 December 2021; accepted manuscript online 7 January 2022)

Here, simultaneous *in-situ* calibration of pressures and temperatures was performed in a hinge-type second-stage cubic large volume press (LVP) up to 15 GPa and 1400 K by an acoustic travel-time approach. Based on the recently reported P–t_S and P–T–t_P–t_S equations for Al_2O_3 buffer rod, the cell pressures and temperatures in the chamber of LVP were *in-situ* determined, in comparison with those by conventional off-line (or fixed-points) pressure calibration method and direct thermocouple measurement, respectively. It is found that the cell pressures of the LVP chamber are significantly reduced after annealing at simultaneous high pressures and high temperatures, owing to the stress relaxation as accumulate in the LVP chamber. This acoustic travel-time method is verified to be a good way for precise determination of thermal (cell) pressures at high temperature conditions, and is of great importance and necessity to conduct *in-situ* physical property measurements under extreme high P–T conditions, especially when the precious synchrotron x-ray/neutron diffraction beams are not available.

Keywords: cubic press, simultaneous *in-situ* calibration of pressures and temperatures, acoustic travel-time, high pressure and high temperature

PACS: 07.35.+k, 91.60.Gf, 91.60.Lj, 43.35.Yb **DOI:** 10.1088/1674-1056/ac4902

1. Introduction

Pressure (P) and temperature (T) are important thermodynamic parameters to modulate structures or physical properties of materials and provide new insights into the nature of matter under extreme P–T conditions.[1,2] To date, large volume press (LVP) has been widely used in industrial applications and scientific research owing to their unique advantages such as large sample volume, precise high-temperature control, and low costs.[3–9] However, only few LVP are installed at synchrotron/neutron sources beamline stations, i.e., beamline-based LVP, and the corresponding cell pressures can be *in-situ* determined by using the equation-of-state (EOS) of pressure markers, such as Au, Pt, MgO, and NaCl.[10–13]

In terms of in-house (laboratory setup) LVP, the LVP cell pressures are usually off-line calibrated at room temperature as a function of ram load, which inevitably yields relatively large errors especially for the simultaneous high P–T calibrations. Cell pressures at room temperature are usually calibrated by the electrical resistance method, based on the well-known fixed-points phase transition of some typical materials upon compression (e.g., Bi, Tl, Ba, ZnTe, and ZnS).[5,8,14,15] By contrast, the cell pressures at high temperatures are usually calibrated by the recovered minerals/material subjected to olivine-to-wadsleyite or quartz-to-coesite phase transitions at high pressure and high temperature, which are usually identified using x-ray diffraction measurements and/or scanning electron imaging (SEM) observations,[16,17] or by the melting curve of metals (i.e., Cu and Al) at high pressure.[18] For conventional/off-line pressure calibration methods, however, the high-pressure cell assembly is needed to put pressure marks/materials, so those methods are not suitable to determine cell pressures at simultaneous high-temperature and high-pressure conditions. As a result, those traditional off-line pressure calibration methods are not suitable or precise enough for *in-situ* physical property measurements (i.e., electrical resistivity measurements, and ultrasonic measurements), owing to relatively larger errors in the calibrated cell pressures at simultaneous high-pressure and high-temperature conditions. Thus, precise calibrations of cell pressures and/or temperatures are of necessity and importance for carrying out high-pressure and/or high-temperature experiments when synchrotron x-ray/neutron diffraction beams are not available.

Recently, new methods for *in-situ* pressure calibration by using an acoustic travel-time approach have been further developed by some groups. Wang *et al.*[19] firstly reported that the shear wave travel-times of Al_2O_3 buffer rod can be utilized for *in-situ* determination of pressures and temperatures in a LVP chamber up to 15 GPa and 900 °C. Higo *et al.*[20] and Song *et al.*[21] have also performed the cell pressure calibration in a large volume press by calibrating the travel-times of Al_2O_3 buffer rod at pressures up to 12 GPa and room temperature. The previous results from acoustic-calibration method are in good agreement with those by fixed-points room-temperature pressure calibration results. On the other hand, temperatures in LVP are usually directly measured by using thermocouples (e.g., $Pt_{94}Rh_6$/$Pt_{70}Rh_{30}$, and

[†]Corresponding author. E-mail: flmyaya2008@163.com

© 2022 Chinese Physical Society and IOP Publishing Ltd

$W_3Re_{97}/W_{25}Re_{75}$). During LVP-based high P–T experiments, an additional electromotive force (EMF) can be induced by many factors such as pressures, and thermocouple position, resulting in inaccuracy of measurements.[1] In this method, thermocouples are usually placed on the surface of tungsten carbide anvils to reduce the deformation upon compression, but still have a risk to breakdown the thermocouples at high pressure, and should destroy the integrity of the heater and chamber when the thermocouple was placed on the cell assembly.

The hinge-type cubic large volume press, also called China-type cubic large volume press, as a type of important high-pressure device, has been widely used in industrial synthesis and high pressure scientific research both in China and world.[5,8] On the basis of the previous study on the ultrasonic travel-time of polycrystalline Al_2O_3 versus pressures and temperatures,[19] we have performed simultaneous *in-situ* calibration of pressures and temperatures in the hinge-type second-stage cubic large volume press up to 15 GPa and 1400 K. The pressures and temperatures in a LVP chamber are *in-situ* and simultaneous determined to be independent of synchrotron x-ray/neutron diffraction beams, as compared with those by conventional/offline pressure calibration method and direct thermocouple measurements, respectively. The precise calibration of pressures at variously high temperatures in a LVP is reported.

2. Experimental methods

High pressure ultrasonic measurement experiments were conducted in a newly designed hinge-type cubic large volume press (6×14 MN) with second-stage, which was installed at the high-pressure laboratory of China Mianyang Research Reactor (CMRR) neutron scattering facility, China Academy of Engineering Physics.[22–26] The schematic experimental setup for the newly designed hinge-type cubic LVP, and the high-pressure ultrasonic measurement system is shown in Fig. 1.

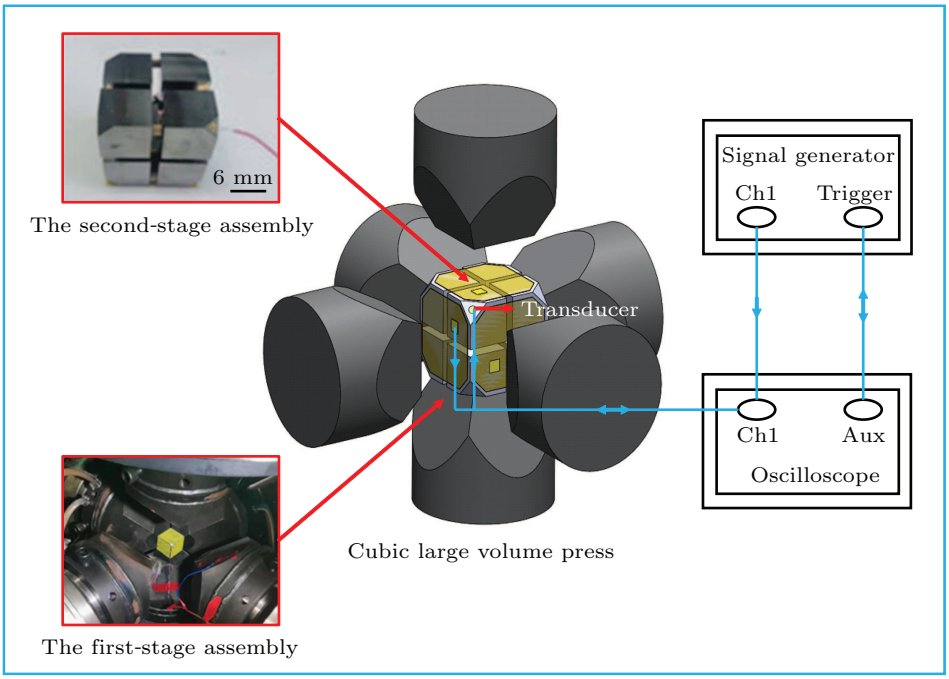


Fig. 1. The schematic experimental setup for the hinge-type cubic LVP-based high pressure ultrasonic measurement system.

The corresponding cell assemblies for the current LVP-based ultrasonic measurement at high P and high/room T are shown in Fig. 2. The 14/8 cell assembly, an MgO octahedron with the edge length of 14 mm as a pressure medium and eight cubic WC anvils with the truncation edge length of 8 mm as the second-stage anvils, is used. A high-density double-side polished of polycrystalline Al_2O_3 and WC are served as acoustic buffer rod and the sample respectively. For simultaneously high P–T ultrasonic measurements, the sample is usually surrounded by a mixture of NaCl and hexagonal boron nitride (h-BN) (4:1 by weight), which can provide a quasi-hydrostatic pressure environment around the sample. The quasi-hydrostatic environment of the cell has been verified in previous h-AlN compression experiments.[23] A gold foil with 2 μm thickness is inserted between the buffer rod and the sample to enhance their mechanical coupling. In terms of high temperature experiments, a rhenium foil with 50 μm thickness is used as a furnace/heater to generate high temperatures. A W_3Re_{97}–$W_{25}Re_{75}$ thermocouple is placed near the sample side for direct measurements of the cell temperatures. The acoustic signals are excited by a dual mode $LiNbO_3$ transducer (10-degree Y-cut), serving as both a transmitter and receiver,

which is mounted on the back corner of one WC cube. During the current ultrasonic measurements, the compressional (P) and shear (S) wave travel-times are derived by using the pulse echo overlap (PEO) technique,[27] and the travel-times inside the Al_2O_3 buffer rod and the sample were obtained by overlapping the echoes reflected from the anvil and the buffer rod with a precision better than 0.2%.[28–30]

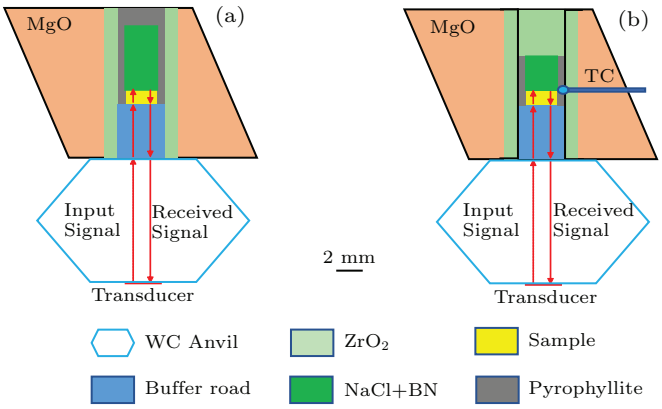


Fig. 2. Schematic cross-section cell assemblies for the current LVP-based ultrasonic measurements at (a) high-P and room T; (b) and at the simultaneous HP and HT conditions.

3. Results and discussion

In this experiment, we have performed five heating-cooling cycles at ram loads up to 3.46 MN and temperatures up to 1400 K. In the current high P–T acoustic experiments, all the data are collected along cooling during decompression. The as-measured sample is annealed at the peak pressures and temperatures for several minutes to release nonhydrostatic stress accumulated in the sample upon compression. Figure 3 shows the typical acoustic echoes at the peak pressure and temperature of ∼ 15 GPa and ∼ 1400 K from the current LVP-based ultrasonic measurements at high pressure and high temperature. The high signal-to-noise ratio and the clear separation of reflections from the buffer rod and the sample ensure a precise determination of travel-times of the sample.

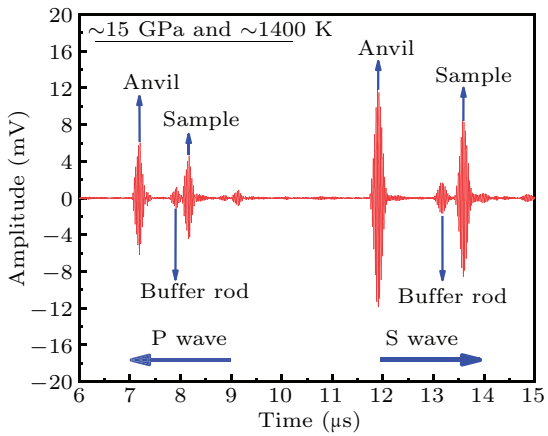


Fig. 3. Typical acoustic echoes of the interfaces between the WC anvil, Al_2O_3 buffer rod, and a typical WC sample at ∼ 15 GPa and ∼ 1400 K.

3.1. *In-situ* calibration of pressures at room temperature

As shown in Table 1, the shear waves travel-times (t_S) for Al_2O_3 buffer rod at different ram loads from the ultrasonic measurements at high pressure and room temperature (runs 1 and 2) are summarized. The cell pressures as a function of ram loads can be derived, based on the previously reported P–t_S relation of Al_2O_3 buffer rod[19]

$$P\,(\mathrm{GPa}) = 249.7\,(7) \times (1 - t_S/t_{S0})\,, \qquad (1)$$

where t_S and t_{S0} are the S wave travel-times at high pressure and zero pressure, respectively. t_{S0} is derived from a least square fit of t_S in this study. Although the Al_2O_3 buffer rod is not located at the center of the high P–T cell assembly which may cause nonnegligible nonhydrostatic stress accumulated in the buffer rod, by using the current acoustic pressure–temperature calibration method, the accumulated stress in the buffer rod will have no effect on the calibrated pressure and temperature results. Because we have used the same high P–T cell assembly as Wang *et al.*,[19] where the P–t_S and P–T–t_P–t_S equations are derived based on the measured travel-times for Al_2O_3 buffer rod, and the cell pressures from the synchrotron x-ray diffraction date of pressure markers for NaCl or Au (located at the center of the chamber). Details can be found elsewhere in Ref. [19].

Table 1. Shear wave travel-times of Al_2O_3 buffer rod at various ram loads from the current high-pressure ultrasonic measurements for runs 1 and 2.

Run 1		Run 2	
F (MN)	$2t_S$ (μs)	F (MN)	$2t_S$ (μs)
0.0	1.2256(2)	0.0	1.2460(2)
0.43	1.2130(2)	0.69	1.2256(2)
0.98	1.1960(2)	0.97	1.2162(2)
1.21	1.1886(2)	1.66	1.1998(2)
1.48	1.1828(2)	1.94	1.1948(2)
1.69	1.1772(2)	2.22	1.1888(2)
1.94	1.1732(2)	2.59	1.1838(2)
2.19	1.1692(2)	2.77	1.1812(2)
2.49	1.1634(2)	3.05	1.1774(2)
2.77	1.1604(2)	3.39	1.1736(2)
2.94	1.1578(2)	3.60	1.1716(2)
3.19	1.1554(2)	3.88	1.1688(2)
3.46	1.1528(2)		

For comparison, the corresponding room temperature cell pressures are also calibrated by using the well-known phase transition of some typical materials (e.g., Bi: I–II at 2.55 GPa; ZnTe: I–II at 5 GPa, II–III at 9–9.5 GPa, semi/metal at 11.5–13 GPa; ZnS: semi/metal at 15.6 GPa), i.e., fixed-point pressure calibration method. For good understanding, the cell pressures as determined by our measured shear wave travel-times for Al_2O_3 buffer rod are plotted as a function of ram load in Fig. 4, as compared with those by the conventional off-line pressure calibration method. It can be seen, the cell pressures as *in-situ* determined from the acoustic travel-time method are in good agreement with those by the conventional fixed-point method within mutual uncertainties.

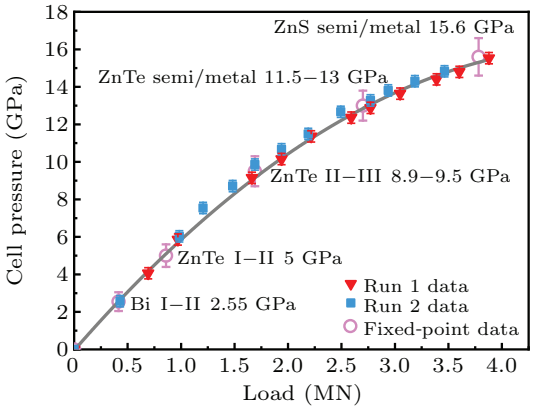


Fig. 4. *In-situ* ultrasonic calibration of pressures at room temperature in a hinge-type LVP, the gray line is a guide to the eye.

3.2. *In-situ* calibrations of temperatures and pressures

As reported in Ref. [19], the cell pressure and temperature can both be determined by P and S wave travel-times (t_P and t_S), profit from the P and S waves can be measured simultaneously by the state-of-the-art ultrasonic measurement technique, and the P–t_P–t_S and T–t_P–t_S equations can be expressed as

$$P(\mathrm{GPa}) = -245.4(\pm3.4)\times(1-t_S/t_{S0}) + 402.7(\pm2.1)\times(1-t_P/t_{P0}), \quad (2)$$

$$T(K) = 300-44278.2(\pm353.6)\times(1-t_S/t_{S0}) + 36496.0(\pm2.1)\times(1-t_P/t_{P0}), \quad (3)$$

where t_S/t_P is the measured S/P wave travel-time at high pressure, and t_{S0}/t_{P0} is at zero pressure. Since both P and S waves are simultaneously measured in the current study, and the intrinsic difference between P and S waves in their respective pressure and temperature dependences warrants a unique solution for pressure and temperature. The measured t_S/t_P and the determined pressure and temperature at various high P–T are summarized in Table 2. For comparison, temperatures directly measured by thermocouples are also included. t_{S0} and t_{P0} were derived from a least square fit of t_S and t_P at high pressure of various ram load and the temperature annealing to ambient, and yield to 0.6882 μs and 1.1806 μs, respectively. What is noteworthy is that, in some cases, the buffer rod may experience plastic deformation if the stress exceeds the yield strength of polycrystalline Al_2O_3 during heating to the peak pressure and temperature conditions of the experiment in the first heating cycle. However, if the subsequent heating along decompression is not above the peak temperature, the cell assembly is expected to experience only elastic deformation, thus the results of pressure and temperature calibration are also believable.

Table 2. Summary of acoustic travel-times (t_P and t_S), ram load, electric power, temperatures, and pressures as calibrated by acoustic travel-time method and direct thermocouple measurements.

F (MN)	Power (W)	t_P (μs)	t_S (μs)	T^a_{Tc} (K)	$T^b_{acoustic}$ (K)	$P^c_{acoustic}$ (GPa)
3.46	500	0.6692(2)	1.1858(2)	1358	1390	11.8(2)
3.46	450	0.6680(2)	1.1770(2)	1182	1197	11.2(2)
3.46	400	0.6662(2)	1.1684(2)	1048	1061	10.9(2)
3.46	300	0.6634(2)	1.1580(2)	806	813	10.4(2)
3.46	200	0.6610(2)	1.1488(2)	603	609	9.9(2)
3.46		0.6576(2)	1.1376(2)	300	300	9.2(2)
2.77	500	0.6720(2)	1.1892(2)	1364	1407	11.2(2)
2.77	450	0.6702(2)	1.1810(2)	1197	1225	10.6(2)
2.77	400	0.6686(2)	1.1730(2)	1061	1064	10.0(2)
2.77	300	0.6660(2)	1.1608(2)	813	821	9.8(2)
2.77	200	0.6636(2)	1.1532(2)	609	619	9.1(2)
2.77		0.6601(2)	1.1402(2)	300	300	8.7(2)
2.08	500	0.6754(2)	1.1942(2)	1375	1420	10.3(2)
2.08	450	0.6738(2)	1.1858(2)	1224	1246	9.8(2)
2.08	400	0.6722(2)	1.1786(2)	1064	1081	9.1(2)
2.08	300	0.6694(2)	1.1656(2)	829	837	9.0(2)
2.08	200	0.6672(2)	1.1582(2)	621	629	8.2(2)
2.08		0.6634(2)	1.1446(2)	300	300	7.7(2)
1.38	450	0.6782(2)	1.1926(2)	1244	1261	8.6(2)
1.38	400	0.6760(2)	1.1848(2)	1098	1110	8.2(2)
1.38	300	0.6734(2)	1.1724(2)	842	856	7.9(2)
1.38	200	0.6708(2)	1.1640(2)	631	633	7.1(2)
1.38		0.6668(2)	1.1506(2)	300	300	6.4(2)
0.69	450	0.6908(2)	1.2104(2)	1268	1290	5.0(2)
0.69	400	0.6892(2)	1.2042(2)	1120	1139	4.6(2)
0.69	300	0.6860(2)	1.1928(2)	864	885	4.2(2)
0.69	200	0.6828(2)	1.1824(2)	655	668	3.8(2)
0.69		0.6780(2)	1.1654(2)	300	300	3.5(2)

[a]The temperatures were measured directly by thermocouple.
[b]The temperatures were determined by acoustic travel-time method.
[c]The pressures were determined by acoustic travel-time method.

To further confirm the validation of acoustic high *P*–*T* calibration approach, the temperatures *versus* powers at different ram load are plotted in Fig. 5(a), as compared with those by direct thermocouple measurements. Obviously, the temperatures obtained from the acoustic travel-time approach are generally consistent with those by direct thermocouple measurements. However, the temperatures measured by thermocouples are slightly lower than those calibrated by acoustic travel-time method, especially at high temperature region. This discrepancy may be due to the effects of pressure and temperature on the electromotive force (EMF) when performing direct temperature measurements by using thermocouples. This behavior has been reported where the difference between the nominal and real temperatures was ∼ 29 K at 16 GPa and 1173 K, and this difference will become much more pronounced at higher temperatures and pressures.[31]

To clarify the effects of various pressures on temperatures at a certain electric power, various temperatures as a function of ram loads at electric powers of 300 W and 450 W are shown in Fig. 5(b), which is *in situ* calibrated by acoustic travel-time approach. It is easy to see that the pressure effects on the temperature cannot be ignored, due to the cell assembly/heater is deformation and shrink during the compression. The temperatures are ∼ 20 °C/MN drops when the ram loads increase from 0.5 MN to 3.5 MN.

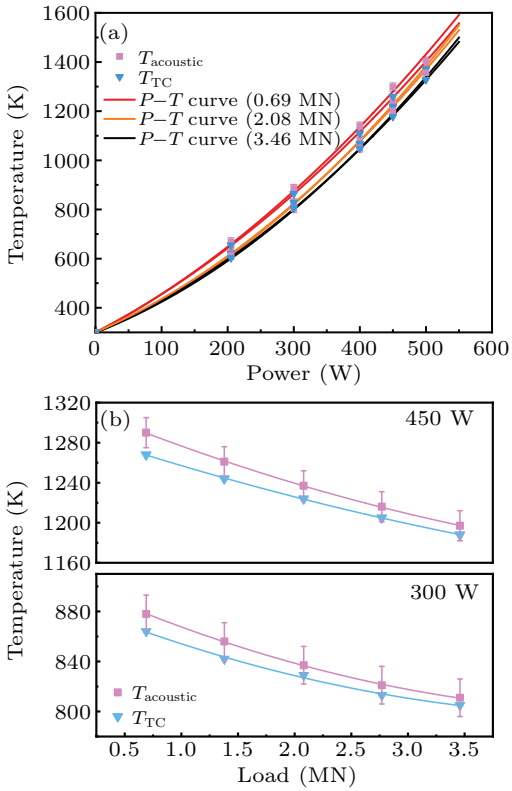


Fig. 5. (a) Temperatures versus powers at various load. (b) Pressure effect on the temperature as calibrated by acoustic travel-time approach, in comparison with those by direct thermocouple measurements.

To know deeply about stress accumulated in high-pressure cell assembly during cold compression, the *in-situ* calibration of cell pressures before- and after-annealing are plotted in Fig. 6(a) for comparison. It is found that the cell pressure drops about 30% (from ∼ 14 GPa to ∼ 10 GPa) at the same load of 3.5 MN just after annealing at ∼ 1400 K, owing to the stress relaxation at high temperature. In order to further know how temperature affects the cell pressures after annealing in the LVP-based high *P*–*T* experiments, the cell pressures are plotted as a function of temperature and load in Fig. 6(b). It finds that the cell pressures show an increase of ∼ 0.2 GPa with the increase of temperatures by 100 K after annealing. To conclude, at a certain load, the cell assembly up to a maximum pressure before annealing at maximum temperature, and then the pressure will decrease with the temperature anneal, and the pressure reach a minimum when the temperature anneal to ambient.

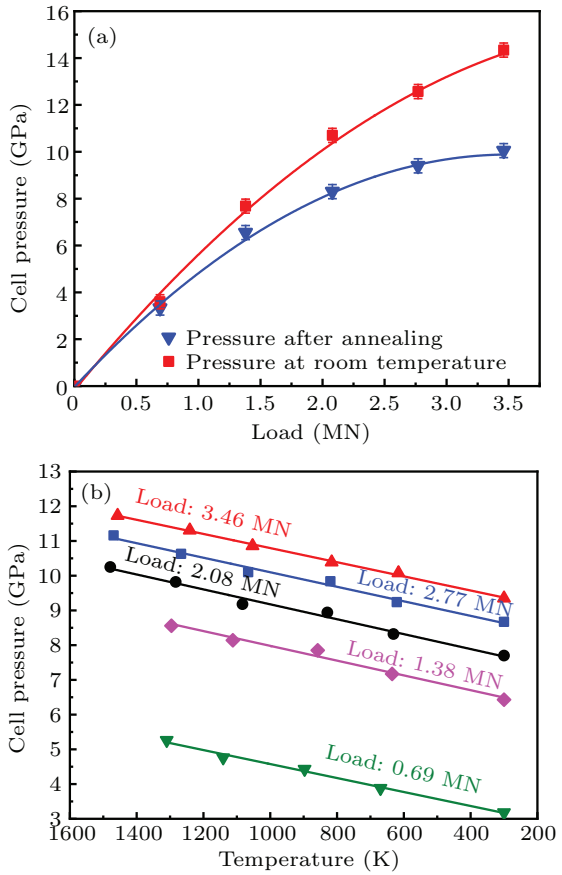


Fig. 6. (a) Ambient-temperature cell pressures versus load after annealing, as compared with those before heating; (b) cell pressures as a function of temperature and load.

Based on the current ultrasonic travel-time calibrations of *P*–*T* results, an empirical formula to determining the cell pressures (*P*) by a two-dimensional temperature–load (*T*–*F*) can be yielded,

$$P\,(\mathrm{GPa}) = 5.60 \times F - 0.80 \times F^2 + 0.002 \times (T - 300)\,, \quad (4)$$

where F is the load in MN, and T is the temperature in K.

The obtained empirical formula is helpful to understand the rear pressure of the cell assembly in LVP high *P*–*T* ex-

periments. Indeed, this empirical formula cannot be commonly used in all cell assembly, because the formula should be changed by the change of cell assembly materials and *P–T* experiment region. However, its significance is to know how the cell pressure changes and *in-situ* determine the pressure and temperature in LVP high *P–T* experiments by acoustic travel-time method.

4. Conclusion

In this study, ultrasonic interferometry measurement system has been performed into a hinge-type second-stage cubic large volume press (LVP), in order to *in-situ* simultaneous calibration of pressures and temperatures up to 15 GPa and 1400 K by using acoustic travel-time approach. The results show that the acoustic travel-time *in-situ* pressure-calibration approach is much more convenient and reliable and can be used for both room-temperature pressure calibration and simultaneous high *P–T* calibration, and the calibrated temperatures by acoustic travel-time approach agree well with those by direct thermocouple measurements. An empirical formula for pressure is presented to understand the rear pressure of the cell assembly in LVP high *P–T* experiments. The significance of acoustic travel-time *P–T* calibration approach is to know how the cell pressure changes and *in-situ* determine the pressure and temperature in LVP high *P–T* experiments. This method can be conducted *in-situ* physical property measurements under extreme high *P–T* environments and can be used in different type of LVP, especially when the rare synchrotron x-ray/neutron diffraction beams are not available.

Acknowledgements

The authors would like to thank Prof. Yongtao Zou, Prof. Duanwei He and Prof. Fang Peng for the helpful discussions.

Project supported by the National Natural Science Foundation of China (Grant Nos. 12075215, 11872198, and U2030110) and the National Key Research and Development Program of China (Grant No. 2016YFA0401503).

References

[1] Sokol A G, Borzdov Y M, Palyanov Y N and Khokhryakov A F 2015 *High Pressure Res.* **35** 139
[2] Frost D J, Poe B T, Nnes R G, Liebske C, Duba A and Rubie D C 2004 *Phys. Earth Planet. Inter.* **143** 507
[3] Takayuki I, Liu Z D and Katsura T 2019 *Engineering* **5** 434
[4] Xie L, Yoneda A, Yoshino T, Yamazaki D, Tsujino N, Higo Y and Ito E 2017 *Rev. Sci. Instrum.* **88** 093904
[5] Fang L M, He D W, Chen C, Ding L Y and Luo X J 2007 *High Pressure Res.* **27** 367
[6] Katsura T, Yamada H, Nishikawa O, Song M, Kubo A, Shinmei T and Funakoshi K I 2004 *J. Geophys. Res.* **109** B02209
[7] Higo Y, Irifune T and Funakoshi K 2018 *Rev. Sci. Instrum.* **89** 014501
[8] Zhang J W, He D W, Fang L M, Hu Q W, Li X, Li Q, Wang J P and Wang Y P 2020 *Rev. Sci. Instrum.* **91** 125103
[9] Shang Y C, Shen F R, Hou X Y, Chen L Y, Hu K, Li X, Liu R, Tao Q, Zhu P W, Liu Z D, Yao M G, Zhou Q, Cui T and Liu B B 2020 *Chin. Phys. Lett.* **37** 080701
[10] Decker D L 1971 *J. Appl. Phys.* **42** 3239
[11] Anderson O L, Isaak D G and Yamamoto S 1989 *J. Appl. Phys.* **65** 1534
[12] Dorfman S M, Prakapenka V B, Meng Y and Duffy T S 2012 *J. Geophys. Res.* **117** B08210
[13] Dorogokupets P I and Oganov A R 2007 *Phys. Rev. B* **75** 024115
[14] Bean V E, Akimoto S, Bell P M, Block S, Holzapfel W B, Manghnani M H, Nicol M F and Stishov S M 1986 *Physica B+C* **139** 52
[15] Xu C, He D W, Wang H K, Wang W D, Tang M J and Wang P 2014 *Chin. Sci. Bull.* **59** 5251
[16] Decker D, Bassett W A, Merrill L, Hall H T and Barnett J D 1972 *J. Phys. Chem. Ref. Data* **1** 773
[17] Fei Y, Ricolleau A, Frank M, Mibe K, Shen G and Prakapenka V B 2007 *Proc. Natl. Acad. Sci. USA* **104** 9182
[18] Bohlen S R and Boettcher A L 1982 *J. Geophys. Res.* **87(B8)** 7073
[19] Wang X B, Chen T, Qi X T, Zou Y T, Kung J, Yu T, Wang Y B, Liebermann R C and Li B S 2015 *J. Appl. Phys.* **118** 065901
[20] Higo Y, Inoue T, Li B S, Irifune T and Liebermann R C 2006 *Phys. Earth Planet. Inter.* **159** 276
[21] Song W, Shan S M, Tang Q Z, Su C and Liu Y G 2021 *Acta Geochim.* **40** 525
[22] Fang L M, Chen X P, Xie L, He D W, Hu Q W, Li X, Jiang M Q, Sun G A, Chen B, Peng S M, Li H and Han T X 2020 *Chin. J. High Pressure Phys.* **34** 050104
[23] Xu C W, Li Y, Inoue T, Gréaux S, Li Q Z, Gao J, Sun F X and Fang L M 2021 *High Pressure Res.* **41** 233
[24] Li Q Z, Yang X X, Peng F, Yang G Z, Han T X, Fang L M, Hu Q W, Xie L, Chen X P and Zou Y T 2021 *J. Eur. Ceramic Soc.* **41** 4788
[25] Wu B B, Lei L, Zhang F, Tang Q Q, Liu S, Pu M F, He D W, Xia Y H, Fang L M, Ohfuji H and Irifune T 2021 *Matter Radiat. Extreme* **6** 038401
[26] Liang H, Fang L M, Guan S X, Peng F, Zhang Z G, Chen H H, Zhang W and Lu C 2021 *Inorg. Chem.* **60** 515
[27] Li B S, Jackson I, Gasparik T and Liebermann R C 1996 *Phys. Earth Planet. Inter.* **98** 79
[28] Li B S, Kung J, Liu W and Liebermann R C 2014 *Phys. Earth Planet. Inter.* **228** 63
[29] Cai N, Chen T, Qi X T and Li B S 2018 *J. Appl. Phys.* **124** 185901
[30] Gieske J H and Barsch G R 1968 *Phys. Status Solidi* **29** 121
[31] Nishiharav Y, Doi S, Kakizawa S, Higo Y and Tange Y 2019 *Phys. Earth Planet. Inter.* **298** 106348